

## Efficient charge injection from a high work function metal in high mobility n-type polymer field-effect transistors

M. Caironi, C. Newman, J. R. Moore, D. Natali, H. Yan et al.

Citation: *Appl. Phys. Lett.* **96**, 183303 (2010); doi: 10.1063/1.3424792

View online: <http://dx.doi.org/10.1063/1.3424792>

View Table of Contents: <http://apl.aip.org/resource/1/APPLAB/v96/i18>

Published by the [American Institute of Physics](http://www.aip.org).

---

### Related Articles

Ultra-low resistance ohmic contacts in graphene field effect transistors

*Appl. Phys. Lett.* **100**, 203512 (2012)

Three-dimensional distribution of Al in high-k metal gate: Impact on transistor voltage threshold

*Appl. Phys. Lett.* **100**, 201909 (2012)

Electric field effect in graphite crystallites

*Appl. Phys. Lett.* **100**, 203116 (2012)

Efficient terahertz generation by optical rectification in Si-LiNbO<sub>3</sub>-air-metal sandwich structure with variable air gap

*Appl. Phys. Lett.* **100**, 201114 (2012)

Vertically integrated submicron amorphous-In<sub>2</sub>Ga<sub>2</sub>ZnO<sub>7</sub> thin film transistor using a low temperature process

*Appl. Phys. Lett.* **100**, 203510 (2012)

---

### Additional information on *Appl. Phys. Lett.*

Journal Homepage: <http://apl.aip.org/>

Journal Information: [http://apl.aip.org/about/about\\_the\\_journal](http://apl.aip.org/about/about_the_journal)

Top downloads: [http://apl.aip.org/features/most\\_downloaded](http://apl.aip.org/features/most_downloaded)

Information for Authors: <http://apl.aip.org/authors>

## ADVERTISEMENT



**Goodfellow**  
metals • ceramics • polymers • composites  
70,000 products  
450 different materials  
**small quantities fast**

[www.goodfellowusa.com](http://www.goodfellowusa.com)

## Efficient charge injection from a high work function metal in high mobility *n*-type polymer field-effect transistors

M. Caironi,<sup>1,2,a)</sup> C. Newman,<sup>3</sup> J. R. Moore,<sup>1</sup> D. Natali,<sup>2,4</sup> H. Yan,<sup>3</sup> A. Facchetti,<sup>3</sup> and H. Sirringhaus<sup>1</sup>

<sup>1</sup>*Cavendish Laboratory, J. J. Thomson Avenue, Cambridge CB3 0HE, United Kingdom*

<sup>2</sup>*Center for Nano Science and Technology, IIT@PoliMi, Via Pascoli 70/3, 20133 Milano, Italy*

<sup>3</sup>*Polyera Corporation, 8045 Lamon Avenue, Skokie, Illinois 60077, USA*

<sup>4</sup>*Politecnico di Milano, D.E.I., Piazza L. da Vinci 32, 20133 Milano, Italy*

(Received 8 January 2010; accepted 13 April 2010; published online 5 May 2010)

We demonstrate efficient electron injection from a high work function metal in staggered transistors based on the high mobility poly{[*N,N'*-bis(2-octyldodecyl)-naphthalene-1,4,5,8-bis(dicarboximide)-2,6-diyl]-alt-5,5'-(2,2'-bithiophene)}. Channel length scaling shows that the linear mobility for electrons remains higher than 0.1 cm<sup>2</sup>/V s when reducing the channel length to a few micrometers. Field-enhanced injection favors downscaling at a fixed lateral voltage and reduces the contact resistance to 11 kΩ cm at high gate voltages for channels of only a few micrometers. The contacts are asymmetric, with the source contribution dominating the overall resistance, consistent with an injection limited regime rather than bulk-limited as generally found in staggered transistors. © 2010 American Institute of Physics. [doi:10.1063/1.3424792]

In organic field-effect transistors (FETs) ohmic injection is difficult to achieve because of finite Schottky barriers at the metal-semiconductor interface<sup>1</sup> and the difficulty of implementing local doping in the vicinity of the contacts.<sup>2</sup> Apart from a few exceptions,<sup>3</sup> realization of low contact resistance devices usually relies on matching the metal work function ( $W_f$ ) and the frontier molecular energy levels of the semiconductor. Especially in the case of *n*-channel semiconductors the injection of carriers into the lowest unoccupied molecular orbital (LUMO), which usually lies at energies close to or higher than  $-4$  eV,<sup>4-6</sup> often enforces the adoption of reactive metals or of contact modification through self-assembled monolayers.<sup>7</sup> Besides interface physics, the device architecture plays a major role in determining the contact resistance. In staggered configurations such as top-gate/bottom-contact (TGBC) or bottom-gate/top-contact (BGTC), injection is favored by current-crowding effects.<sup>8</sup> The lowest contact resistances for solution processed *n*-channel devices have been reported so far in BGTC FETs, where the direct evaporation of contacts on top of the semiconductor reduces the injection barrier.<sup>9</sup> In this case a value, normalized to the channel width ( $R_c \times W$ ), as low as 2.2 kΩ cm was demonstrated in devices based on a fullerene derivative.<sup>10</sup> To date there are only few reports<sup>11</sup> on contact resistance in solution processed *n*-channel polymeric TGBC FETs.

Recently, a breakthrough in the development of solution processable, *n*-channel organic semiconductors was achieved with the demonstration of poly{[*N,N'*-bis(2-octyldodecyl)-naphthalene-1,4,5,8-bis(dicarboximide)-2,6-diyl]-alt-5,5'-(2,2'-bithiophene)} [P(NDI2OD-T2)] (Polyera ActivInk™ N2200), which exhibits electron mobilities higher than 0.1 cm<sup>2</sup>/V s.<sup>12</sup> In this case Au contacts in a TGBC architecture were adopted and, despite the nominal energy difference between Au  $W_f$  (4.7–5.1 eV) and P(NDI2OD-T2) LUMO level [ $-3.9$  eV (Ref. 13)], good electron injection was observed. However, only long channel

FETs ( $L=50-100$  μm) were reported and little is known about the contact resistance for shorter channel lengths and its physical origin. Here we report on high mobility P(NDI2OD-T2) FETs with channel lengths as short as a few micrometers and we carefully characterize the contact resistance using various methods. Solvent-cleaned Au allows efficient electron injection even in 3.5 μm channel devices, where electron mobilities  $>0.1$  cm<sup>2</sup>/V s are achieved. The contact resistance  $R_c$  in these devices was independently extracted with a channel scaling approach based on the gated transfer line method [gTLM (Ref. 14)] and with a recently developed fully analytical differential method [DM (Ref. 15)]. A gated four-point probe (gFPP) approach was also adopted to discern between the contributions of the source and drain electrodes and to investigate the origin of contact resistance. Our results show that the contact resistance between Au and P(NDI2OD-T2) in a TGBC FET architecture is as low as 11 kΩ cm, one of the lowest values reported so far for solution processed *n*-channel FETs, especially in a bottom-contact configuration. Interestingly,  $R_c$  is found to be dominated by the resistance at the injecting contact (source) and shows a nonlinear dependence with the lateral field.

Alkali-free 1737F glass slides were used as substrates. 15–20 nm Au contacts on a 0.7 nm Cr adhesion layer were patterned by lithography. Au contacts were cleaned in a 2-propanol ultrasonic bath for 2 min. P(NDI2OD-T2) was dissolved in anhydrous 1,2-dichlorobenzene at 120 °C in a glovebox for 20–30 min to obtain a 9 g/l solution. The solution was then filtered through a 0.2 μm PTFE filter and deposited in a glove-box by spin-coating at 1000 rpm for 90 s. The samples were then annealed for 13–15 h at 110 °C on a hot plate. A ~400–500 nm thick layer of CYTOP CTL-809M (Asahi Glass) was deposited by spin-coating in air at 9000 rpm with a 15 s acceleration ramp. After annealing on a hot plate in a glove box at 110 °C for 5 h, a 20 nm-thick Al gate electrode was thermally evaporated. A postannealing of 10 h at 110 °C in a glove box followed. We found that long annealing steps enable high data reproducibility. In the case

<sup>a)</sup>Electronic mail: mario.caironi@iit.it.

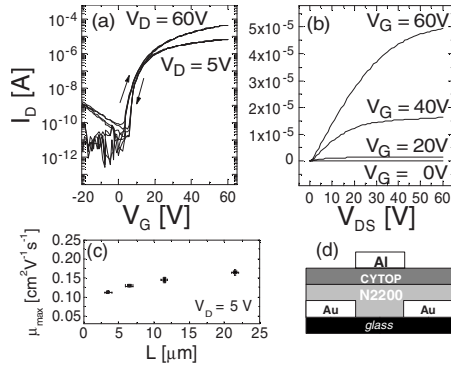


FIG. 1. (a) Transfer and (b) output curves for a P(NDI2OD-T2) FET with  $L=21.5 \mu\text{m}$  and  $W=1 \text{ mm}$ . (c) Linear  $\mu_e$  vs  $L$ . (d) Schematic cross-section of a FET.

of gFPP the semiconductor was patterned into an active layer island by means of a photo-patterning technique<sup>16</sup> which does not affect the device performance. Vertical diodes were prepared by spin-coating a  $\sim 160 \text{ nm}$  P(NDI2OD-T2) layer from xylene on an  $30 \text{ nm}$  Al layer evaporated on glass, and completed by depositing a  $100 \text{ nm}$  thick Al counter-electrode. Electrical measurements were performed at room temperature in a nitrogen atmosphere.

P(NDI2OD-T2) FETs with Au source and drain contacts show very good  $n$ -channel behavior, with transfer curves [Fig. 1(a)] characterized by very low hysteresis. The typical maximum field-effect mobility for electrons ( $\mu_e$ ), extracted from gradual channel approximation equations without taking into account contact resistances effects, are in the range of  $0.2\text{--}0.3 \text{ cm}^2/\text{V s}$  in the saturation regime ( $V_D=60 \text{ V}$ ) and  $0.1\text{--}0.2 \text{ cm}^2/\text{V s}$  in the linear regime ( $V_D=5 \text{ V}$ ), in agreement with previous results.<sup>12</sup> Even for channels as short as a few micrometers an apparent linear  $\mu_e$  in the range of  $0.1 \text{ cm}^2/\text{V s}$  is found, a quite remarkable value for a polymer  $n$ -channel FET with high work-function metal contacts, suggesting an overall very limited contact resistance. From a channel length ( $L$ ) scaling study, a weak apparent dependence of  $\mu_e$  with  $L$  in the linear regime was measured, with  $\mu_e$  decreasing from  $0.15\text{--}0.20 \text{ cm}^2/\text{V s}$  for  $L > 20 \mu\text{m}$  to about  $0.11 \text{ cm}^2/\text{V s}$  for  $L=3.5 \mu\text{m}$  [Fig. 1(c)]. This apparent small decrease in linear  $\mu_e$  with  $L$  in short channels is a clear effect of contact resistances. In fact, a device with  $L=21.5 \mu\text{m}$  shows good output characteristics [Fig. 1(b)], although a very slight deviation from ideality can be observed at small  $V_{DS}$ .

To provide a quantitative analysis of  $R_C$  we first used gTLM for a set of devices with  $L=21.5, 11.5, 6.5,$  and  $3.5 \mu\text{m}$ . The data indicate a  $V_G$  dependent contact resistance  $< 8 \text{ k}\Omega \text{ cm}$  for  $V_G=60 \text{ V}$  [Fig. 2(a)]. This is obtained with air-exposed, solvent cleaned Au contacts [ $W_f=4.7\text{--}4.9 \text{ eV}$  (Ref. 11)], while  $\text{O}_2$  plasma cleaned Au [ $W_f=5\text{--}5.5 \text{ eV}$  (Ref. 11)] affords highly degraded and less reproducible FET characteristics. The latter devices are severely contact limited and do not show a clear scaling with  $L$ . Thus, in the following we only discuss the more interesting case of solvent cleaned contacts.

To gain more insight, we investigated whether  $R_C$  is affected by lateral field enhancement effects, in which case the contact resistance would depend on  $L$ , since  $V_D$  is kept constant at  $5 \text{ V}$  for the various  $L$ . Since gTLM assumes  $R_C$  to be independent of  $L$ , it cannot be used in this context. Thus, a

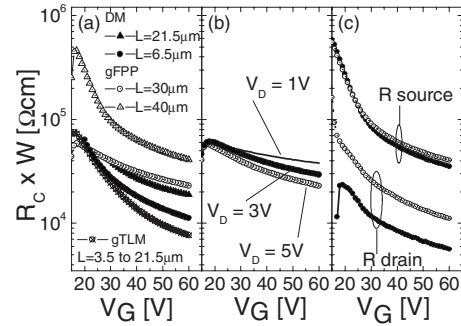


FIG. 2. (a)  $R_C \times W$  at  $V_D=5 \text{ V}$  as a function of  $V_G$  as obtained with various methods. (b)  $R_C \times W$  extracted with gFPP at  $V_D=1, 3,$  and  $5 \text{ V}$  for a device with  $L=30 \mu\text{m}$ . (c)  $R_S \times W$  and  $R_D \times W$  for a device with  $L=40 \mu\text{m}$  measured at  $V_D=5 \text{ V}$  with gFPP, with a first source/drain contacts configuration (black circles) and with swapped contacts (white circles).

fully analytical method<sup>15</sup> is employed. Assuming  $R_C = \alpha(V_G - V_T)^{-1} + R_{C0}$ , where  $\alpha$  is a free parameter,  $V_T$  is the transistor threshold voltage, and  $R_{C0}$  is independent from  $V_G$ , we can extract  $R_{C0}$  by analyzing *individually* the transfer characteristic curves from each channel length. To compare this method with gTLM, the gateable part of the contact resistance is also extracted. The extracted dependence on  $V_G$  is qualitatively similar to the one found with gTLM [Fig. 2(a)], but now a dependence of  $R_C$  on  $L$  is revealed, originating from a dependence of  $R_{C0}$  on the electric field. In fact, for  $V_G=60 \text{ V}$ ,  $R_C$  is as low as  $11 \text{ k}\Omega \text{ cm}$  for  $L=6.5 \mu\text{m}$  (with  $R_{C0}=1.5 \text{ k}\Omega \text{ cm}$ ), but almost doubles for  $L=21.5 \mu\text{m}$  (with  $R_{C0}=8.5 \text{ k}\Omega \text{ cm}$ ).<sup>17</sup>

Since the dependence on the lateral field may change if the contact acts as a charge injector or collector, it is important to distinguish the source and drain contributions. We therefore performed gFPP measurements in devices with two narrow probes ( $2\text{--}3 \mu\text{m}$ ), each at one third of the total channel length, slightly protruding ( $\leq 50 \mu\text{m}$  over a total  $W$  of  $1 \text{ mm}$ ) into the channel.<sup>18</sup> In this way, thanks to a recently developed gFPP method,<sup>8</sup> it is possible to obtain an almost direct measurement of the voltage drop at each contact with high accuracy. The measurements were performed on devices with longer channels ( $L=30\text{--}40 \mu\text{m}$ ) for ease of device fabrication and to reduce the fraction of  $L$  occupied by the two probes. The total  $R_C$  obtained with gFPP shows a gate dependence that for  $V_G > 30 \text{ V}$  is very similar to what was obtained with the previous two methods [Fig. 2(a)]. The dependence of  $R_C$  on  $V_G$ , commonly observed in staggered device configurations, is due to the combined effect of an increase in the effective contact injection area ( $A_{\text{inj}}$ ) due to current-crowding effects<sup>19</sup> and an increase in the polymer bulk conductivity with increasing gate voltage.<sup>8</sup> Both effects can be accounted for by combining a current-crowding model and a  $V_G$  dependent bulk conductivity as previously reported,<sup>8</sup> resulting in a characteristic dependence of  $R_C$  on  $V_G$ . However in the present case the effective injection length  $L_T$ , the fraction of the total physical contact over which the injection is spread, calculated with the analytical expression provided in the paper by Chiang *et al.*,<sup>19</sup> shows less than 10% variation as a function of  $V_G$  for  $V_G > 30 \text{ V}$  and fixed  $V_D$  of  $5 \text{ V}$ . In this range  $L_T$  varies between  $9.2$  and  $10 \mu\text{m}$  and  $1.3$  and  $1.6 \mu\text{m}$  for the source and the drain contacts, respectively, compared to a gate-to-contact overlap of  $20 \mu\text{m}$  for each electrode. Correspondingly  $A_{\text{inj}}=W \times L_T$  is almost constant and therefore as a first approximation  $R_C$

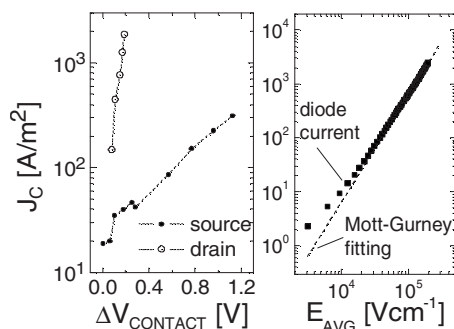


FIG. 3. (a) Current density at the source and at the drain contacts vs the corresponding voltage drop at  $V_G=60$  V. (b)  $J$  vs the average applied field in a Al/P(NDI2OD-T2)/Al diode (squares) and best fitting to Mott–Gurney law by assuming a dielectric constant of 3 (dashed line).

$\propto (V_G - V_T)^{-1}$ .<sup>8,19</sup> The latter expression corresponds to the simple gate dependence assumed in the case of DM, validating its adoption. Furthermore, the lateral field dependence of  $R_C$  is unambiguously confirmed with gFPP [Fig. 2(b)]. Above  $V_G=40$  V the contact resistance extracted for a drain voltage of  $V_D=5$  V is consistently lower than that extracted at  $V_D=1$  V. A value of  $\sim 23$  k $\Omega$  cm is obtained at  $V_G=60$  V and  $V_D=5$  V for  $L=30$   $\mu$ m. This is higher than values from gTLM reflecting the reduced lateral field in the longer channel gFPP measurements. Importantly, the source resistance ( $R_S$ ) is generally higher than the drain resistance ( $R_D$ ) by approximately four to seven times [Fig. 2(c)]. Moreover, when the two contacts are swapped, the measured  $R_S$  is only slightly affected, while  $R_D$  varies substantially. This is probably due to small morphological differences in the semiconductor close to the contacts. These findings suggest that  $R_S$  is limited by the reverse biased Schottky barrier at the source metal–semiconductor interface while at the forward biased drain junction the resistance becomes dominated by the transport through the bulk. This explains why morphological differences in the semiconductor close to the contact do not produce a variation in  $R_S$ , where the injection is strongly dominated by the interface. On the other hand, at the drain contact resistance is dominated by transport through the bulk, thus the higher sensitivity of  $R_D$  to small physical differences in the contact region.

To provide a better description of the injection we compared the dependence of the channel current on the voltage drop at the source and drain contacts ( $\Delta V_S = I_D \times R_S$  and  $\Delta V_D = I_D \times R_D$ , respectively) using the data obtained with gFPP. Since  $L_T$  varies significantly as a function of  $V_D$ , for each  $\Delta V_S$  and  $\Delta V_D$  we calculated the actual  $A_{inj} = W \times L_T$ . In this way it is possible to plot the current density at the contacts ( $J_C$ ) versus the relative voltage drop [Fig. 3(a)]. The drain contact shows a higher current density for the same voltage drop, reflecting the lower contact resistance. It is noticeable that at the drain the slope of the curve is much higher than at the source. This different field enhancement reflects the different origin of the resistance at the two contacts, as discussed before. A more in-depth analysis would be needed to precisely determine the injection and extraction mechanisms since the system is complicated by a nonlinear combination of gateable and nongateable contributions<sup>8</sup> at both contacts and of a bulk and an interface contribution at the source. Nevertheless, our study clearly demonstrates a source-drain asymmetry of the contact resistance in P(NDI2OD-T2) transistors, a feature which is not usual in

staggered architectures,<sup>8</sup> where the bulk contribution usually plays a major role. In the P(NDI2OD-T2) system the source contact resistance is higher due to the contribution of the metal-organic interface, which dominates the overall  $R_C$ . On the other hand the bulk contribution is small, as demonstrated by the very low value of the drain resistance of a few k $\Omega$  cm, reflecting a high bulk conductivity. This is confirmed by electrons only vertical diodes, where for an average applied field in the  $10^4$ – $10^5$  V cm<sup>-1</sup> range, comparable to the field at the drain contact in the linear regime, the current is space-charge limited and follows very well the Mott–Gurney law,<sup>20</sup> from which we can extract a relatively high bulk mobility in the range of  $0.5$ – $1 \times 10^{-3}$  cm<sup>2</sup>/V s [Fig. 3(b)].

In conclusion, solution processed *n*-channel P(NDI2OD-T2) FETs, with a bottom-contact staggered configuration and Au contacts, show a surprisingly low contact resistance of  $\sim 10$ – $20$  k $\Omega$  cm despite the presence of an energetic barrier for injection at the source contact.  $R_C$  depends on the lateral field, which is a limiting factor but favors injection in the shorter channels and explains the relatively high mobility of  $>0.1$  cm<sup>2</sup>/V s for channels only a few micrometers long. The total contact resistance is dominated by the source component in agreement with an injection-limited regime. Our work quantifies the contact resistance in high-mobility *n*-channel polymeric FETs with high work-function metal contacts suggesting that polymers such as P(NDI2OD-T2) are strong candidates for the development of high performance complementary circuits.

M.C. thanks Dr. J.-F. Chang for assistance with patterning and Dr. T. Sakanoue and Dr. X. Cheng for useful discussions; M.C. and D.N. thank Dr. L. Fumagalli for his help with DM. We thank Z. Chen of Polyera Corporation for ActivInk™ N2200 synthesis. The research has been supported by the Cambridge Integrated Knowledge Center (CIKC) and the Engineering and Physical Sciences Research Council (EPSRC).

<sup>1</sup>L. Bürgi *et al.*, *J. Appl. Phys.* **94**, 6129 (2003).

<sup>2</sup>B. A. Gregg *et al.*, *Chem. Mater.* **16**, 4586 (2004).

<sup>3</sup>M. Kitamura *et al.*, *Appl. Phys. Lett.* **93**, 033313 (2008).

<sup>4</sup>C. R. Newman *et al.*, *Chem. Mater.* **16**, 4436 (2004).

<sup>5</sup>J. Zaumseil and H. Sirringhaus, *Chem. Rev. (Washington, D.C.)* **107**, 1296 (2007).

<sup>6</sup>H. Usta *et al.*, *J. Am. Chem. Soc.* **131**, 5586 (2009).

<sup>7</sup>S. Braun *et al.*, *Adv. Mater. (Weinheim, Ger.)* **21**, 1450 (2009).

<sup>8</sup>T. J. Richards and H. Sirringhaus, *J. Appl. Phys.* **102**, 094510 (2007).

<sup>9</sup>P. V. Pesavento *et al.*, *J. Appl. Phys.* **96**, 7312 (2004).

<sup>10</sup>S. P. Tiwari *et al.*, *J. Appl. Phys.* **106**, 054504 (2009).

<sup>11</sup>X. Cheng *et al.*, *Adv. Funct. Mater.* **19**, 2407 (2009).

<sup>12</sup>H. Yan *et al.*, *Nature (London)* **457**, 679 (2009).

<sup>13</sup>Z. Chen *et al.*, *J. Am. Chem. Soc.* **131**, 8 (2009).

<sup>14</sup>S. Luan and G. W. Neudeck, *J. Appl. Phys.* **72**, 766 (1992).

<sup>15</sup>D. Natali *et al.*, *J. Appl. Phys.* **101**, 014501 (2007).

<sup>16</sup>J.-F. Chang *et al.*, *Adv. Funct. Mater.* (to be published).

<sup>17</sup>Due to  $L$  dependence of  $R_{C0}$ , gTLM is strictly not applicable, even though the error is limited on the shortest channels where the total resistance is dominated by the gateable part. Since  $R_{C0}$  is assumed to be  $V_G$ -independent in DM, its dependence on  $L$  can be unambiguously attributed to a dependence on the electric field.  $V_T$  dependence on  $L$  only affects the gate-voltage dependent term. In our case  $V_T$  was equal to 12 V, 14.5 V, and 15.3 V for  $L=6.5$   $\mu$ m, 11.5  $\mu$ m, and 21.5  $\mu$ m, respectively. Likely due to short channel effects, the DM method could not be applied for  $L=3.5$   $\mu$ m.

<sup>18</sup>R. J. Chesterfield *et al.*, *J. Appl. Phys.* **95**, 6396 (2004).

<sup>19</sup>C.-S. Chiang *et al.*, *Jpn. J. Appl. Phys., Part 1* **37**, 5914 (1998).

<sup>20</sup>N. F. Mott and R. W. Gurney, *Electronic Processes in Ionic Crystals* (Oxford University Press, London, 1940).